

# Harnessing Algal Biomass: Superabsorbent and Biostimulant Hydrogels for Seed Germination in Soilless Cultivation

Camilla Febo,\* Manuela Ciocca, Mauro Maver, Tanja Mimmo, Oussama Bouaicha, Luigimaria Borruso, Paolo Lugli, Luisa Petti, Athanassia Athanassiou,\* and Danila Merino\*

**ABSTRACT:** Hydrogels are emerging as sustainable alternatives to petroleum-based foams and pots in horticulture due to their high porosity, enhancing water and nutrient retention. This study develops  $\kappa$ -carrageenan (Carr)-based hydrogels incorporating hydrolyzed (HSW) and nonhydrolyzed red seaweed (WSW) (0–50 wt %) to introduce biostimulant properties for soilless cultivation. Hydrogels were analyzed for swelling in different media, solubility, microstructure (SEM), physicochemical interactions (FTIR, XRD), and mechanical properties, revealing high porosity, superabsorbent behavior (swelling up to 6000%), and reduced compression modulus with increasing seaweed content. Their biostimulant effect was assessed on *Arabidopsis thaliana*, with 20 wt % HSW hydrogels promoting enhanced root and shoot growth. Additionally, the hydrogels inhibited *Fusarium solani*, demonstrating antifungal properties. These results highlight the potential of Carr-seaweed hydrogels as multifunctional substrates for sustainable plant cultivation.

**KEYWORDS:** superabsorbent hydrogels, biostimulants, seaweed, sustainability, soilless

## 1. INTRODUCTION

Agriculture is one of the most resource-intensive sectors, requiring significant amounts of water and land for cultivation.<sup>1,2</sup> As urbanization accelerates, innovative strategies to enhance crop yields and bring food production closer to cities become imperative.<sup>3</sup> Hydroponics, a leading soilless cultivation method, provides precise control over environmental factors such as nutrient levels, pH, temperature, and light.<sup>4</sup> However, conventional hydroponic substrates, typically composed of synthetic foams, plastics, rockwool, peat moss, and other materials, are often expensive, imported, and environmentally problematic.<sup>5</sup> In particular, peat extraction has significant ecological consequences, underscoring the need for sustainable alternatives.<sup>6</sup>

An ideal substrate should possess specific morphological characteristics such as high porosity, robust physical support, and excellent water retention capacity.<sup>7</sup> While no universal substrate exists, biobased materials like hydrogels are emerging as promising alternatives. Hydrogels are three-dimensional hydrophilic networks of polymer chains that can be cross-linked by physical or chemical bonds.<sup>8</sup> Biobased hydrogels are particularly suitable for horticulture, offering optimal mechanical support to plants, high water retention, and minimal environmental impact as reported for starch/ethyl cellulose, chitosan/citric acid/urea, guar gum/succinic anhydride and other carbohydrate type polymers.<sup>9</sup> Moreover, they can serve multiple roles, including soil conditioning,<sup>10</sup> seed coating, and mulch films, often in combination with biostimulants to enhance plant growth.<sup>11–13</sup>

Plant biostimulants are compounds or microorganisms that, when applied to plants, enhance natural plant processes such as stress resistance and nutrient efficiency.<sup>14</sup> They serve as

sustainable alternatives to chemical fertilizers, which can adversely affect water, air, and soil quality.<sup>15</sup> Among these, seaweed extracts are widely recognized sustainable biostimulants.<sup>16</sup> Derived from various algae and microalgae, including brown, red, and green species, seaweed extracts have demonstrated biostimulant effects on both edible and non-edible plants by activating defense mechanisms,<sup>17</sup> increasing resistance to stress<sup>18</sup> and promoting growth through the secretion of auxins and cytokinins.<sup>19</sup> Additionally, they provide antifungal activity against pathogens<sup>20</sup> such as *Fusarium oxysporum* and *Rhizoctonia solani*, which affect crops like tomato, soybean, and pepper.<sup>21–23</sup>

In this study, the red seaweed *Chondrus crispus* (*C. crispus*), commonly known as “Irish moss”, is used as a filler in hydrogels prepared from  $\kappa$ -carrageenan (Carr) biopolymer to develop biostimulant substrates for seed germination and plant growth in soilless cultivations. While *C. crispus* biostimulant properties require further comprehensive study, recent studies have shown its ability to enhance drought tolerance in tomato plants,<sup>24</sup> alleviate salinity stress in *Vicia faba*,<sup>25</sup> and improve turnip greens productivity.<sup>26</sup> *C. crispus* contains, on average, 40–50 wt % carbohydrates, 1–3 wt % lipids, 10–38 wt % minerals, and about 27% proteins (dry weight).<sup>27,28</sup> Interestingly, Carr, the main polysaccharide extracted from *C. crispus*, is a high-molecular-weight sulfated galactan capable of forming

**Received:** November 13, 2024

**Revised:** June 3, 2025

**Accepted:** June 5, 2025

high-swelling hydrogels.<sup>29</sup> Its structure consists of linear chains of galactose and 3,6-anhydrogalactose with alternating  $\alpha$ -(1 → 3) and  $\beta$ -(1 → 4) linkages, and it is classified into  $\lambda$ -,  $\iota$ -, and  $\kappa$ -carrageenan based on the number and position of sulfate groups.<sup>30</sup>

By integration of the biostimulant properties of *C. crispus* with the structural benefits of Carr hydrogels, this study develops a sustainable soilless substrate. We demonstrate that *Arabidopsis thaliana* seeds germinate successfully in hydrogels containing 20% hydrolyzed seaweed, producing plants with a biomass 502% higher than that grown in carrageenan-only hydrogels. These results highlight the potential of seaweed-based hydrogels to enhance plant growth and promote sustainable agricultural practices.<sup>31</sup>

## 2. MATERIALS AND METHODS

**2.1. Materials.** K-Carrageenan was purchased from Sigma-Aldrich, molecular weight 453–652 kDa (St. Louis, MO, USA). Commercial raw and dried Irish moss was purchased from Neulabs srl (Milano, MI, IT). *Arabidopsis thaliana* Col-0 seeds were provided by the Competence Centre for Plant Health (Bolzano, BZ, IT). Deionized water was used throughout the preparation of the K-Carrageenan hydrogels (Carr) and of the nonhydrolyzed seaweed solution (WSW), while  $\text{NH}_4\text{OH}$  purchased from Sigma-Aldrich (28%  $\text{NH}_4\text{OH}$  in  $\text{H}_2\text{O}$ ,  $\geq 99.99\%$ ) was used for the preparation of the hydrolyzed (HSW) seaweed solution. KCl, also from Sigma-Aldrich (ACS reagent, 99.0–100.5%), was used to cross-link the films. A fertilizer solution was prepared using 0.5 mL of Flora Gro “Tripart Grow” (GHE Terra Aquatica srl) liquid fertilizer diluted in 1 L of  $\text{dH}_2\text{O}$ , the composition of the liquid fertilizer includes 3% of N, 1% of P, and 6% of K.

**2.2. Preparation of  $\kappa$ -Carrageenan-Seaweed Composite Hydrogels.** The seaweed was received dried, but it was further dehydrated in an oven at 40 °C for 24 h. After that, it was blended in an Oster Versa 1400 (Milwaukee, Wisconsin, US) blender and finally sieved in an Endecott’s Sieve Shaker Minor 200 (London, UK) to obtain a fine powder with a maximum particle size of 50  $\mu\text{m}$ .

Hydrolysis of seaweed was performed according to the method previously reported for other biomasses after minor modification.<sup>32</sup> The required amount of seaweed powder was incorporated into  $\text{NH}_4\text{OH}$  1 M, at a concentration of 5 wt %, stirred at 30 °C and 400 rpm for 4 h. The WSW was instead prepared by dissolving the same seaweed powder in deionized water at the same conditions as the HSW.

Simultaneously, a 2 wt % Carr solution was prepared by dissolving the polymer in deionized water at 80 °C for 2 h. Then, specific volumes of the Carr solution were mixed with different volumes of the HSW and WSW solutions. The mixtures were heated at 80 °C and stirred at 300 rpm for 15 min for a uniform blend. Subsequently, the solutions were poured into Teflon Petri dishes and left in an oven at 30 °C for 72 h to allow the solvent to evaporate and the film to dry. A control consisting of Carr without seaweed addition was also prepared. Once the solvent evaporated, the films obtained were cross-linked for 5 min in a 2 wt % solution of KCl, and then dried again on a heating plate at 40 °C.

The final compositions of the hydrogels and their nomenclatures are indicated in Table 1.

**2.3. Characterization of Hydrogels.** **2.3.1. Fourier-Transform Infrared Spectroscopy (FTIR).** Chemical properties of the films were studied on an INVENIO R FTIR instrument (Bruker, Germany) using attenuated total reflectance (ATR) with diamond crystal accessories. The OPUS software was used to acquire the spectra collection, each measured at a resolution of 4  $\text{cm}^{-1}$  and an average of 64 scans acquired in the 4000–400  $\text{nm}$  range.

**2.3.2. X-ray Diffraction (XRD).** XRD patterns were acquired on a PANalytical Empyrean X-ray diffractometer equipped with a 1.8 kW  $\text{CuK}\alpha$  ceramic tube operating at 45 kV and 40 mA and a PIXcel3D 2 × 2 area detector. The diffraction patterns were collected under

**Table 1. Samples Composition with Different Concentrations of Hydrolyzed and Non-Hydrolyzed Seaweed<sup>a</sup>**

Sample's name	Carr (wt %)	HSW (wt %)	WSW (wt %)
Carr	100	0	0
5 CHSW	95	5	0
10 CHSW	90	10	0
20 CHSW	80	20	0
30 CHSW	70	30	0
50 CHSW	50	50	0
5 CWSW	95	0	5
10 CWSW	90	0	10
20 CWSW	80	0	20
30 CWSW	70	0	30
50 CWSW	50	0	50

<sup>a</sup>Abbreviations: Carr: carrageenan; HSW: Hydrolyzed seaweed; WSW: nonhydrolyzed seaweed; CHSW composite with carrageenan and hydrolyzed seaweed; CWSW composite with carrageenan and nonhydrolyzed seaweed.

ambient conditions using a parallel-beam geometry and symmetric reflection mode. Diffractograms were measured in the range of 5–60° (2 $\theta$ ) with a step size of 0.03° and 350 s per step. XRD analysis was performed by using HighScore 4.5 software.

**2.3.3. Scanning Electron Microscopy (SEM) and Energy-Dispersive X-ray Spectroscopy (EDS).** SEM was performed using a SEM JEOL-JSM 6490 (JEOL Ltd., Akishima, Japan) operating at 10–15 kV of accelerating voltage and equipped with an X-ray energy-dispersive detector. The samples were cut after being immersed in liquid nitrogen. Their cross-sectional surface was exposed by adhering the hydrogels to aluminum stubs by using adhesive carbon tape. The exposed surface was then sputtered, forming a layer of 10 nm of gold. The micrographs were captured with a load current of 78  $\mu\text{A}$ , an accelerating voltage of 10–15 kV, and a magnification of 1000 x. The diameter of the pores was calculated using the software ImageJ with the SEM image scale bar as a reference.

**2.3.4. Swelling Ratio.** The swelling ratio of the hydrogels was evaluated in three different media: tap water, deionized water, and a solution with commercial plant fertilizer (diluted 0.5 mL in 1 L of tap water, as suggested by the supplier) to check the possible influence of ions on the swelling degree. To do this, film samples were cut in a circular shape of 6 mm diameter, dried in a vacuum oven at 40 °C for 24 h to define the initial weight ( $W_0$ ), and then swelled in the three media. The swollen weight ( $W_1$ ) was recorded after 24 h. Swelling was calculated as in eq 1.

$$\text{Swelling (\%)} = \frac{W_1 - W_0}{W_0} \times 100 \quad (1)$$

The same process was done to check the rate of hydrogel swelling over 26 h only in the fertilizer solution. In this case, the samples were weighed after 1, 3, 5, 24, and 26 h. The swelling (%) was calculated as in eq 1 for each selected hour. For all of these measurements, each sample was analyzed in triplicate, and results were reported as average  $\pm$  standard deviation (SD).

**2.3.5. Mechanical Properties.** Compression tests were performed on an INSTRON 3365 machine (Instron, UK). The hydrogels were initially swollen in the fertilizer solution and cut in half (5 mm height and 8 mm diameter) to facilitate the analysis. During the experiment, the crosshead speed was set at 3  $\text{mm min}^{-1}$ . The compression modulus (kPa) was measured for all of the samples tested in triplicate. The findings are reported as the mean  $\pm$  SD.

**2.3.6. Biostimulant Effect on Plants.** To evaluate the biostimulant activity of the hydrogels, a growth test was performed using *Arabidopsis* (*A. thaliana*) as a plant model. The schematic setup is shown in Figure 1. The films were cut into 11 mm diameter disks and were put to swell for 5 h in the fertilizer solution. The seeds of *A. thaliana* were sterilized in three steps: first, washing the seeds with a

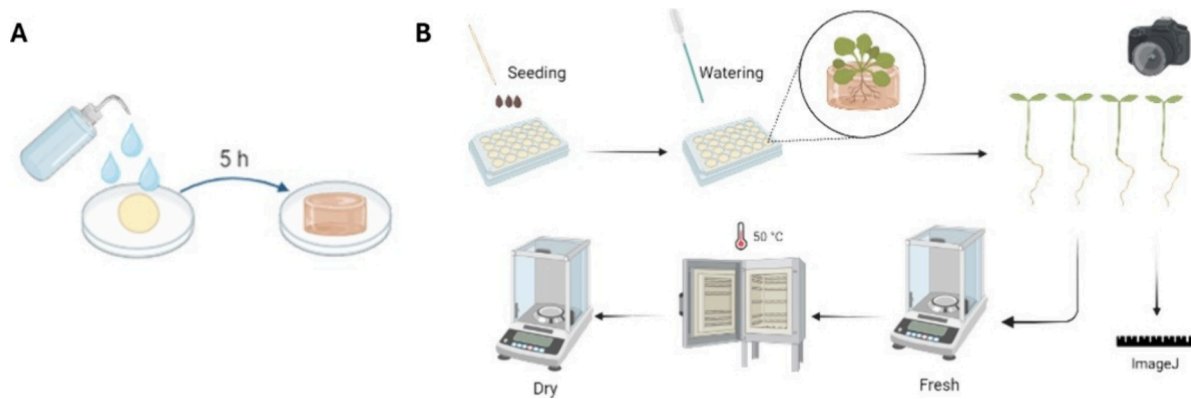


**Figure 1.** Graphical scheme of the setup for the growth test and of the methodology for the analysis. Step (A) swelling of the cut films' disks to obtain hydrogels; step (B) seeding of *A. thaliana* on hydrogels; watering once a week; pictures taken after 14 days of growth; measurements of root length with software; fresh weight; drying for 24 h; dry weight.

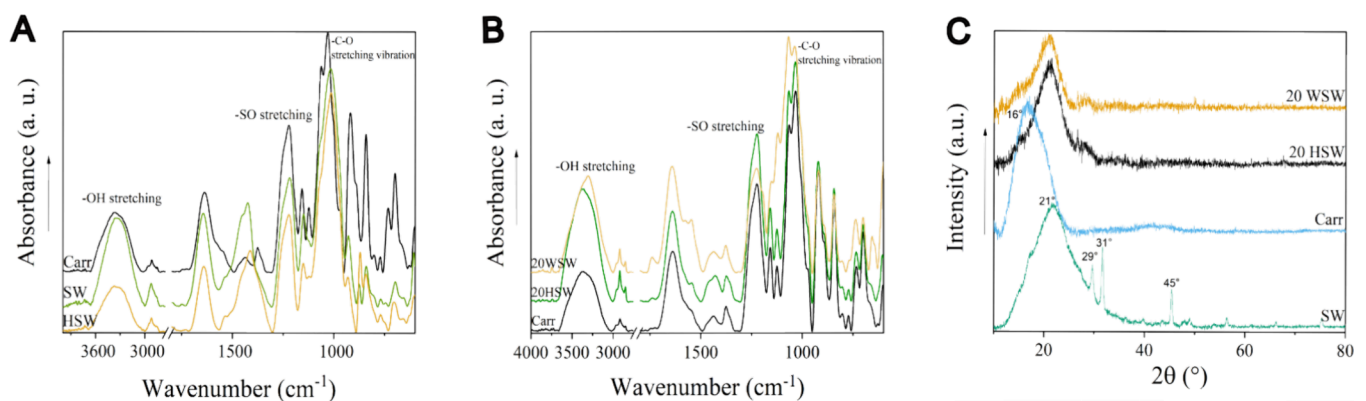


**Figure 2.** Chemical Characterization of Carrageenan Films and Composites, Hydrolyzed Seaweed, and seaweed powder. (A) FTIR spectra of carrageenan film (Carr) (a), raw seaweed powder (SW) (b), and hydrolyzed seaweed (HSW) (c). (B) FTIR spectra of the carrageenan film (Carr) (a), 20 CHSW (b), and 20 CWSW composite (c). (C) XRD patterns of (a) seaweed powder (SW) and carrageenan (Carr) (b).

solution of 70% ethanol +0.1% SDS (sodium dodecyl sulfate), in which the seeds were kept for about 1 min; second, washing the seeds with a 70% ethanol solution, and last, drying the seeds under a laminar flow hood for about 2–3 h after the removal of excess ethanol from the previous steps. At this point, the seeds were sown on top of the hydrogels in the 24 multiwell plates. After *A. thaliana* seeding, the plates were closed and sealed with PARAFILM and placed for stratification at 4 °C for three days. After stratification, the plates were incubated in a growing chamber (GroBanks CLF Plant Climatics) at 22 °C and a day/night cycle of 16/8 h, respectively. The test was conducted for 14 days, and 0.5 mL of fertilizer solution was added only once a week. At the end of the experiment, the seedlings were extracted from the hydrogels, and pictures were taken to analyze with ImageJ software (National Institutes of Health, LOCI, University of Wisconsin). The plants were then weighed both in the fresh and dry weight, and the biomass values were calculated as in eqs 2 and 3.<sup>35</sup> Ten plants for treatment were assayed, giving a total of 130 samples.

$$\text{Increment in fresh weight (\%)} = \frac{W_{f,\text{hydrogel}} - W_{f,\text{control}}}{W_{f,\text{control}}} \times 100\% \quad (2)$$

$$\text{Increment in dry weight (\%)} = \frac{W_{d,\text{hydrogel}} - W_{d,\text{control}}}{W_{d,\text{control}}} \times 100\% \quad (3)$$

where  $W_{f,\text{hydrogel}}$  and  $W_{d,\text{hydrogel}}$  are the fresh and dry weights of plant in the hydrogel, respectively, and  $W_{f,\text{control}}$  and  $W_{d,\text{control}}$  are the fresh and dry weights of plant in the Carr control, respectively.

**2.3.7. Inhibitory Effect of the Hydrogel on the In Vitro Fungi Growth and Spore Germination.** The plant pathogenic fungi *Fusarium solani* was chosen to evaluate the antifungal activity of Carr and CHSW. Carr was considered a control for CHSW material, since it has been reported to be environmentally safe.<sup>34</sup> For the hydrogel, 20 CHSW was chosen as it performed best in terms of plant growth and gel swelling parameters compared to other concentrations of HSW and WSW.

*F. solani* spore germination, elongation, and radial growth in response to 20 CHSW and Carr were assessed according to Bouaicha et al.<sup>35</sup> with some modifications. Briefly, the spore suspension was collected from *F. solani* culture grown on potato dextrose agar (PDA) for five days. The culture was flooded with distilled sterile water, and the surface was scratched gently using a sterilized inoculation loop. The resulting suspension was filtered through sterile gauze and centrifuged at 3500 rpm for 5 min. Next, 1.5 mL of melted hydrogels, obtained by putting Carr and 20 CHSW in Eppendorf and then placed in a hot bath at 90 °C for 2 min, was placed on microscopic slides using sterile polylactic acid molds (20 mm diameter). For mycelium radial growth, 2 μL of fungal spores were pipetted in the center of the media, and the glass slides were incubated in a biological incubator at 26 °C in the dark inside sterile Petri dishes. After 4 days, one picture was taken from each replicate using a camera coupled with a binocular loop (×1), and the colony diameter was evaluated using ImageJ software. The experiment was conducted in six replicates for each material.

The spore germination and hypha extension were measured directly on the slides after 12 h using the same experimental design with some modifications. Ten μL of *F. solani* spore solutions (10<sup>6</sup> spores per mL) were spread on the surface of the melted hydrogels

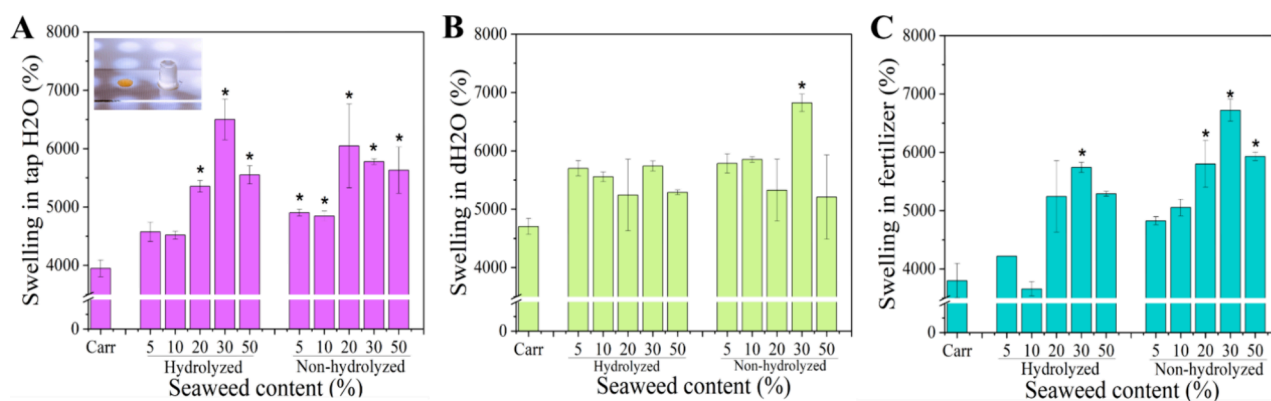


**Figure 3.** Swelling measurements in different media as a function of the different percentages of HSW and WSW and swelling for 24 h. The symbol \* indicates that the results are significantly different according to Tukey's test ( $p < 0.05$ ) compared with the control (Carr). (A) Swelling test in tap water. (B) Swelling test in distilled water. (C) Swelling test in fertilizer solution.

homogeneously. The slides were disposed of in covered Petri dishes and incubated in the dark at 26 °C. We used three replicates for each material. Four pictures were taken from each replicate using a camera coupled to a Leica light microscope ( $\times 20$ ). Finally, utilizing ImageJ software, hypha elongation was measured, and the spore germination rate was calculated.

**2.3.8. Statistical Analysis.** Results are reported as the mean  $\pm$  SD on at least three replicates. To determine if there were significant differences between the means at a 0.05 significance level, one-way analysis of variance (ANOVA) and Tukey's test were conducted in the Origin 2019b (OriginLab, Massachusetts, USA) software.

### 3. RESULTS AND DISCUSSION

#### 3.1. Chemical and Morphological Characterization.

The chemical interactions between the carrageenan polymer and both hydrolyzed and nonhydrolyzed seaweed were comprehensively examined using FTIR and XRD, on the samples in the form of films. Additionally, the morphological characteristics of their bulk microstructure were analyzed through SEM images acquired for the swollen hydrogels.

**3.1.1. FTIR Analysis.** The FTIR spectra of carrageenan, seaweed powder (SW), and hydrolyzed seaweed (HSW) are displayed in Figure 2A. In the SW spectra, it is possible to notice a broad peak between 3000 and 3660  $\text{cm}^{-1}$  and centered at 3340  $\text{cm}^{-1}$  associated with the O–H stretching vibration band given by the hydroxyl group of both the polysaccharides present in the seaweed and the water molecules adsorbed.<sup>36</sup> The band at 1641  $\text{cm}^{-1}$  corresponds to the overlapped carbonyl stretching of amide I in proteins and bending of adsorbed water molecules.<sup>37</sup> The peaks appearing in the 1550–1650  $\text{cm}^{-1}$  are associated with the stretching vibrations of C–H groups present in aromatic compounds.<sup>38</sup> These bands can be attributed to naturally occurring aromatic compounds found in red seaweeds, such as p-coumaric acid, caffeic acid, salicylic acid, hypogallic acid, and chlorogenic acid. Other aromatic compounds that can be related to these bands are flavonoids.<sup>39</sup> The peak at 1426  $\text{cm}^{-1}$  is attributed to the symmetrical bending of  $\text{CH}_2$  typical of cellulose,<sup>40</sup> another polysaccharide present in the seaweed's cell wall. The peaks observed around 1221–1224  $\text{cm}^{-1}$  are attributed to the S–O stretching of the ester sulfate groups present in the polysaccharide Carr.<sup>41</sup>

After hydrolysis, some changes were observed in the positions of the bands of OH, C–OH, and C–O–C (Figure 2A). It is possible to notice in the spectrum of HSW an increase in absorbance in the band centered at 3332  $\text{cm}^{-1}$ ,

when referred to the intensity of the band centered at 2029  $\text{cm}^{-1}$ , associated with the C–H stretching vibrations, and here used as the reference band. Similarly, other changes in the intensity and positions of the bands in the 900–700 and 1300–1000  $\text{cm}^{-1}$  ranges that are associated with the C–O–C group of polysaccharides and the C–OH of carbohydrates were observed after the hydrolysis, which suggests polysaccharide hydrolysis and new hydrogen bond formation.<sup>42</sup>

Additionally, it was observed a shift in the peak position of amide III, from 1426 to 1410  $\text{cm}^{-1}$  that can be attributed to new hydrogen bonding interactions.<sup>43</sup> The Carr film spectrum showed similar peaks to SW and HSW, such as the broad peak centered at 3350  $\text{cm}^{-1}$ , but the peak associated with the cellulose at 1426  $\text{cm}^{-1}$  was not observable here. In addition, a peak observed at 1640  $\text{cm}^{-1}$  is related to the H–O–H bending deformation band (adsorbed water),<sup>44</sup> while the one centered at 1375  $\text{cm}^{-1}$  is related to the ester sulfates<sup>45</sup> as expected for Carr. In addition, the band present at 1157  $\text{cm}^{-1}$  could be assigned to C–O and C–C stretching vibrations of the pyranose ring found in all polysaccharides.<sup>36</sup> Peaks present between 1013 and 1064  $\text{cm}^{-1}$  are both a combination of symmetric and asymmetric stretching mode of C–O–C and the C–O–H of 3,6-anhydro galactose that is one of the main sugars that compose carrageenan.<sup>46</sup> In the fingerprint region (900–750  $\text{cm}^{-1}$ ), the main characteristic peaks of Carr are displayed at approximately 839–841  $\text{cm}^{-1}$  which are assigned to D-galactose-4-sulfate and also the bands at around 919–922  $\text{cm}^{-1}$  confirming the presence of 3,6-anhydro-D-galactose.<sup>47</sup> The peak at 695  $\text{cm}^{-1}$  is assigned to the sulfate on C-4 galactose.<sup>46</sup>

Figure 2B shows the FTIR spectra of two selected samples with 20 wt % of hydrolyzed and nonhydrolyzed seaweed (20 CHSW, 20 CWSW) and Carr for comparison. With the addition of different percentages of HSW and WSW to Carr, some changes were observed (Figure 2B). Concerning CHSW, the peaks related to the O–H stretching (3000–3660  $\text{cm}^{-1}$ ) increased their intensity and broadened, suggesting that HSW increased the H-bonding in the hydrogels.<sup>32</sup> The band at 1375  $\text{cm}^{-1}$  of the ester sulfate is higher in intensity due to an increase of HSW content and the same is noticeable for the band at 1221–1224  $\text{cm}^{-1}$  of the S–O stretching. On the contrary, in the 20 CWSW spectrum, it is possible to notice a decrease in the 3357/3301  $\text{cm}^{-1}$  and the 2916/2917  $\text{cm}^{-1}$  ratio, indicating that in the CWSW the increase in hydrogen bonding is not happening.

Figure S1 shows the spectra obtained for all the films developed (both HSW and WSW), displaying that in the hydrolyzed composites the OH/CH intensity ratio is higher than that in the nonhydrolyzed.

**3.1.2. XRD Analysis.** XRD spectra of red seaweed and Carr are shown in Figure 2C. The SW showed one broad peak centered at  $21^\circ$  with a small shoulder at approximately  $16^\circ 2\theta$ , which may be attributed to the characteristic diffraction peaks of cellulose present in the cell wall of red seaweed.<sup>48</sup> On the other hand, Carr showed only a broad peak centered at  $16^\circ$ , which is attributed to the amorphous nature of the polysaccharide.<sup>49</sup> The spectrum of the red seaweed powder also exhibited sharp peaks at  $2\theta = 29^\circ, 31^\circ,$  and  $45^\circ$  which can be attributed to naturally occurring minerals that comprise approximately 10–38% of the seaweed's total weight. These minerals include silica ( $\text{SiO}_2$ ) and weddellite ( $\text{CaC}_2\text{O}_4 \cdot 2\text{H}_2\text{O}$ ) both previously identified in red seaweeds.<sup>49</sup> The distinct peaks attributed to mineral presence and the peaks associated with cellulose were evident in the XRD patterns of hydrogels containing varying proportions of hydrolyzed and non-hydrolyzed seaweed, as detailed in the Supporting Information (SI 2). Notably, no significant differences were observed in the XRD patterns of hydrogels prepared from hydrolyzed and nonhydrolyzed seaweeds, indicating that the hydrolysis process did not impact the crystallinity of the hydrogels. Besides, the analysis confirms a predominant presence of the amorphous phase, particularly noteworthy given the relatively small proportion of seaweed content, and the cellulose content present in it.

**3.1.3. Swelling of the Developed Hydrogels.** A highly porous structure and a pronounced swelling capacity are ideal characteristics for a material intended to support plant growth.<sup>50</sup> Figure 3A–C show the different swelling behavior of the hydrogels according to their composition in three different aqueous media after 24 h of testing. In tap water (Figure 3A), the swelling percentage of Carr was nearly 4000%, similar to the one reported in the literature,<sup>51</sup> while it reached 6500% for the composites containing HSW and 6000% for the composites with WSW. This exceptional swelling behavior can be attributed to the presence of sulfate groups in Carr and seaweeds, rendering their materials highly hydrophilic.<sup>52</sup> Besides, the increase in swelling after adding the seaweeds agrees with the results of FTIR, suggesting an increase in hydrogels' hydrophilicity (increase in OH availability and hydrogen bonding).<sup>52</sup> As can be appreciated, the addition of seaweed resulted in a significant increase in the swelling percentage of Carr hydrogels, with greater swelling at higher filler content. The increased swelling ability could be explained as the seaweed interaction with Carr partially interferes with Carr assembly and cross-linking thus leaving more OH available to bind water.<sup>53</sup> A similar trend was observed for hydrogels swelled in fertilizer solution (Figure 3C), while a less pronounced difference was noted in the swelling percentage of hydrogels swelled in distilled water ( $\text{dH}_2\text{O}$ ), as shown in Figure 3B. In all cases, the swelling percentages were remarkably high, indicative of the superabsorbent nature of these materials.<sup>54</sup>

It is also worth noting how the films swelled in all of the liquid media tested. It was found that the average thickness of films was around 1 mm, but after absorbing liquid media, the diameter increased from 6 to 8 mm, and the main change was noticed in height, which was 1 cm (Figure 4). As a result, this behavior is mainly influenced by the structure of the network

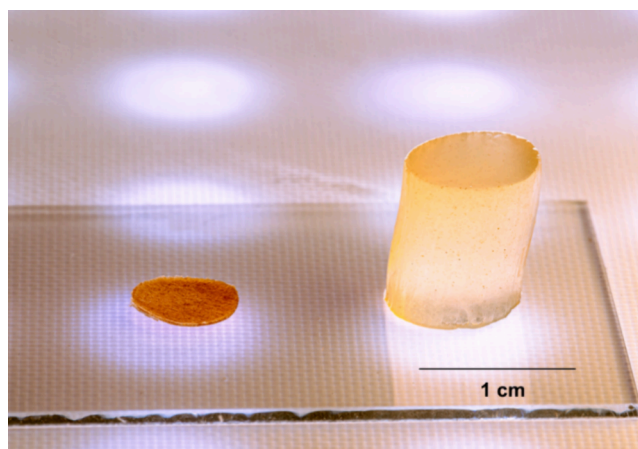


Figure 4. Visual appearance of the 20 CHSW film (left) and then swollen to obtain the hydrogel (right).

and its ability to bind water; actually, it is determined by water diffusion and the formation of ionic bonds between the cross-linking agent and the  $\text{OSO}_3^-$  groups of  $\kappa$ -Carr.<sup>55</sup>

To assess the swelling rate over time, the samples were weighted at intervals of 1, 3, 5, 24, and 26 h after been swelled in the fertilizer solution. As shown in Figure 5, the obtained swelling percentages indicate that the hydrogels typically reach a plateau after the 5 h of immersion in the swelling media.<sup>51</sup> However, exceptions are observed in the samples containing 50 wt % of HSW (Figure 5A) and 30 and 50 wt % of WSW (Figure 5B). This deviation can be attributed to the tendency of these samples to start dissolving in the media, as is visually appreciated.

**3.1.4. SEM and EDS Analysis.** The morphological structure of Carr, CHSW, and CWSW hydrogels was examined by SEM. The SEM pictures of the cross-section of the swollen samples after the freeze-drying process are shown in Figure 6. The Carr matrix appears to be sponge-like with a highly directional porous network (Figure 6A). The addition of HSW or WSW affected the hydrogels' microstructure. In fact, while the hydrogels with lower percentages of HSW and WSW revealed a more defined porous structure (Figure S3A,B), the ones with higher percentages (from 30 to 50%) have bigger and collapsed pores after cutting indicating a more flat and compact composition (Figure S3C,D,G,H). Considering that the hydrogels felt softer after freezing in liquid  $\text{N}_2$ , this may have affected the pores observed after cutting the samples.

Average pores' diameter was calculated using ImageJ software; however, it was not possible to measure it in all the samples due to the previously mentioned collapsed structure after cutting. For Carr, the average pore size was  $116 \pm 5.25 \mu\text{m}$  diameter, and for the samples with 20 HSW,  $315 \pm 11.8 \mu\text{m}$ . The increased porous structure found in 20 CHWS could be significant in the conduction of water and also for nutrient supply to plants, and these characteristics could play a relevant role in soilless cultivation. The EDS spectrum in Figure S4 shows a strong signal for K at 3.5 keV that confirms both the absorption of fertilizer solution by the hydrogel and the cross-linking with KCl.

**3.2. Mechanical Properties of the Developed Swelled Hydrogels.** The mechanical properties upon compression of the hydrogels are depicted in Figure 7. The highest Young's modulus was reached by Carr with a value of 213 kPa, lower than what is reported in the literature.<sup>56,57</sup> This can be related

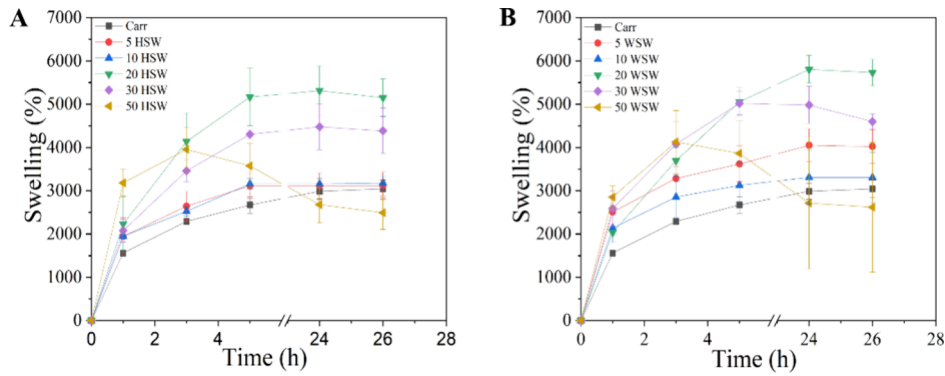


**Figure 5.** Swelling test in fertilizer solution. (A) Curves of swelling (%) vs time (h) for the CHSW set. (B) Curves of swelling vs time for the CWSW set.

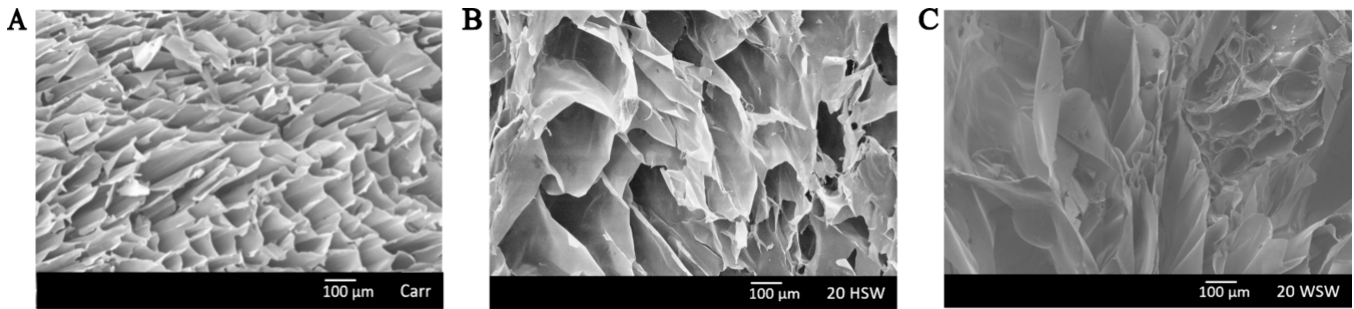


**Figure 6.** SEM micrographs of the freeze-fractured cross-section of (A) Carr, (B) 20 CHSW, and (C) 20 CWSW.

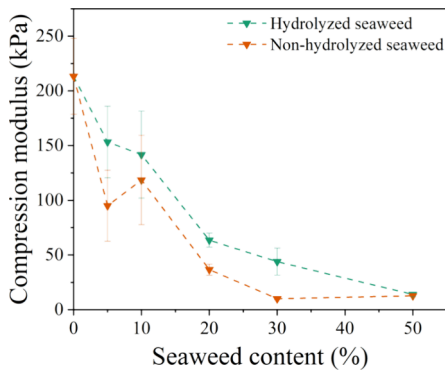


**Figure 7.** Young's modulus (kPa) of Carr-SW based hydrogels with 5, 10, 20, 30, and 50 wt % of HSW and WSW.

to the fact that the cross-linking was done in the film and not in the hydrogel form. The increasing amount of seaweed (from 5 to 50 wt %) within the hydrogels caused a decrease to the Young's modulus, reaching a minimum of 50 kPa in 30 CHSW, and of 10 kPa in 30 CWSW. The hydrolyzed set, overall, showed higher values of modulus compared to the nonhydrolyzed set. Even if hydrolyzed, the presence of seaweed in the particulate form may hinder the formation of a cohesive network within the Carr hydrogel matrix, thereby reducing its modulus. In other words, the dispersed particles of seaweed may disrupt the intermolecular interactions between polymer chains, resulting in a weaker network, as can also be appreciated in the SEM pictures (Figure 6A–C) where it is possible to underline the more directional structure of Carrageenan alone (Figure 6A) compared to the more

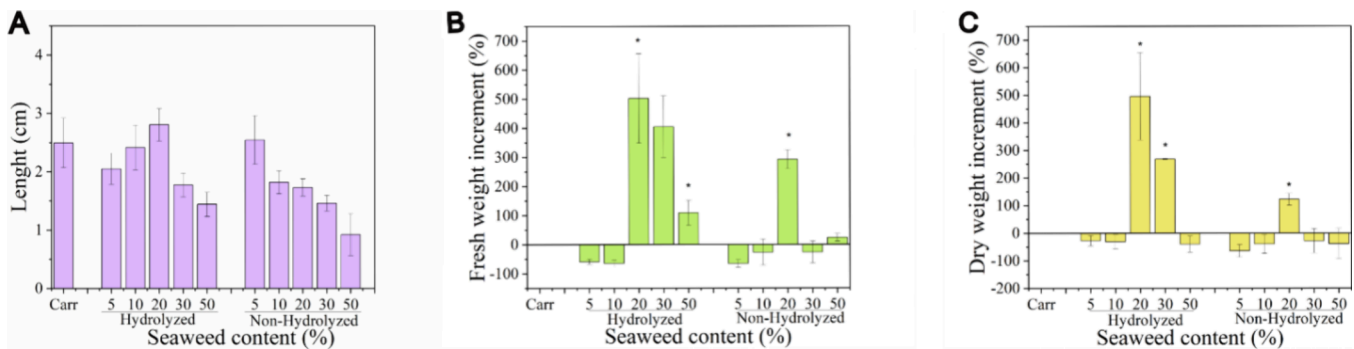


**Figure 8.** Root length and fresh/dry weight percentage variation, with respect to carrageenan, of *A. thaliana* seedlings after 14 days. The symbol \* indicates that the results are significantly different according to Tukey's test ( $p < 0.05$ ) compared with the control (Carr). (A) Root length (cm) as a function of the seaweed percentage in hydrogels for hydrolyzed and nonhydrolyzed sets. (B) Fresh weight percentage variation (%) as a function of the seaweed percentage for both hydrolyzed and nonhydrolyzed sets compared to Carr (C) Dry weight percentage (%) variation measured after 24 h at 50 °C compared to plants grown in Carr.

expanded and less defined of 20 CHSW and 20 CWSW (Figure 6B,C). Moreover, this reduced integrity can lead to increased solubility and susceptibility to dissolution when the hydrogel is exposed to swelling media, as previously shown in Figure 5.

**3.3. Biostimulant Effect on Plants.** The efficiency of the developed hydrogels as substrates for seed germination and plant growth was tested over a period of 14 days using *A. thaliana*. After the 14-day period, the grown plants were harvested, and the length of their roots was measured (Figure 8A). Notably, no significant differences were found between Carr and CHSW or CWSW concerning root length. However, for the hydrolyzed set (CHSW), a major length was reached using the 20 CHSW compared to Carr, with a value of  $2.80 \pm 0.28$  cm. The results indicate that while seaweed provides nutrients to plants, high concentrations can become harmful. Additionally, the carr hydrogel matrix, may lose its structural integrity when overloaded with seaweed, potentially disrupting water channels critical for optimal plant growth. Interestingly, the seedlings grown in the 50 CWSW hydrogels had the smallest root length ( $0.92 \pm 0.36$  cm), with only two out of ten samples being collected at the end of the test. This outcome suggests that the high percentages of WSW create a hostile environment for plant growth, resulting in stunted development and reduced survival rates among the seedlings. The results indicate that while seaweed provides nutrients to plants, high concentrations can become harmful. Additionally, the Carr hydrogel matrix may lose its structural integrity when overloaded with seaweed, potentially disrupting water channels critical for optimal plant growth.<sup>57</sup>

To evaluate the crop growth, the measurement of both fresh and dry weights of the plants is crucial. Fresh weight represents the weight of the plant when harvested including its water content. On the other hand, the difference between the fresh (Figure 8B) and the dry weights (Figure 8C) of plants grown in the composite hydrogels compared to the control Carr provides valuable insights into the developmental stage of the seedlings. Notably, the fresh weight of plants grown in the hydrolyzed set was higher for composites containing more than 10 wt % of HSW. Specifically, these composites produced plants with more than five times the weight of those grown in Carr. Conversely, in the nonhydrolyzed set, the fresh weight of the plants showed a maximum increase of three times compared to those grown in Carr. Regarding the weights after drying in an oven, it was possible to observe that the % increment was confirmed in the samples grown in 20 and 30 CHSW, with values of 495 and 268%, respectively, compared to Carr alone. On the contrary, the samples in 20 and 30 CWSW lost, respectively, -170 and -55% of weight.

To support the analysis just presented, a visual evaluation of the seedlings after 14 days of growth provides valuable insights, as illustrated in Figures 9 and S5. From these pictures, notable differences in the structures of the plants can be observed. The seedlings grown on Carr hydrogels had a standard growth, indicating typical development. Instead, seedlings grown in the 20 CHSW hydrogels displayed a uniform development of the root and apical areas. This suggests a biostimulant effect of the hydrolyzed seaweed solution, enhancing overall seedling growth and vigor, as also demonstrated by the increased fresh and dry weight (Figure 8). On the other hand, the seedlings grown in the 20 CWSW appeared to be less developed, showing a decrease in the plant dimensions (Figure 9C) and signs of flowering under these conditions

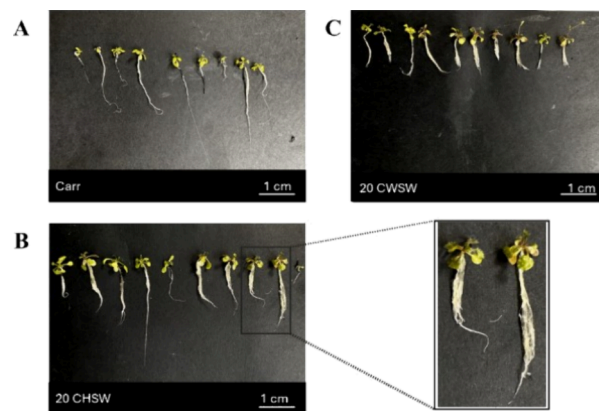


**Figure 9.** Images of *A. thaliana* seedlings grown in Carr (A), in 20 CHSW (B) hydrogels, and in 20 CWSW (C) hydrogels for the visual evaluation of the apical and root development. The scale bar represents 1 cm.

may indicate stress in the plants, as it is often considered an emergency response to environmental challenges.<sup>54,58</sup> These results are promising when compared to other reports in the literature. For example, the work of Teng et al, red cabbage seedling were grown in hydrogels made of agarose enriched with growing mix particles made from processed bark ash and/or coconut coir pith, and the yield of these microgreens increase of only 122% compared to the control.<sup>59</sup> Another study reports the use of chitin hydrogels without the addition of any filler, to be used as substrate for seedling growth of rapeseed, however results showed that plants grown in chitin hydrogels had FW and DW values not significantly different from the ones grown in soil, the only difference was found compared to agar hydrogels.<sup>60</sup> Moreover, cellulose hydrogels with cellulose nanofibers were tested as growth stimulants on black sesame seeds. The germination rate was 100% in four days, and their plants' length presented similar lengths of root and fresh weight compared with soil seedlings.<sup>61</sup>

**3.4. Inhibitory Effect of the Hydrogel on the In Vitro Fungi Growth and Spore Germination.** Both examined materials (i.e., CHSW and Carr) demonstrated minimal fungal mycelium growth (Figure 10D). Although no differences were observed in germ tube elongation (Figure 10A), HSW (20%) significantly decreased radial growth and spore germination rate compared to Carr ( $p < 0.01$ ; Figure 10B,C). These results demonstrate that HSW negatively affected the growth and germination of *F. solani*. Similar studies have shown that several seaweed extracts have antifungal activity against plant pathogenic species such as *F. graminearum*, *F. oxysporum*, and *Aspergillus flavus*.<sup>62</sup> For example, the extract of *Gracilaria edulis* (red seaweed) significantly reduced the radial growth of *Colletotrichum falcatum* compared to the control.<sup>63</sup>

In conclusion, seaweed products can potentially reduce fungal diseases in certain plants, such as carrots and peas, either directly or by boosting plant defense. Therefore, different combinations of seaweed can effectively substitute for traditional pesticides. They offer an environmentally friendly option for controlling plant diseases and are suitable for organic farming.

The present study combined the carrageenan polymer with hydrolyzed and nonhydrolyzed seaweed to form hydrogels as growth substrates for soilless cultivation in sustainable agriculture. The resulting composites exhibited a porous

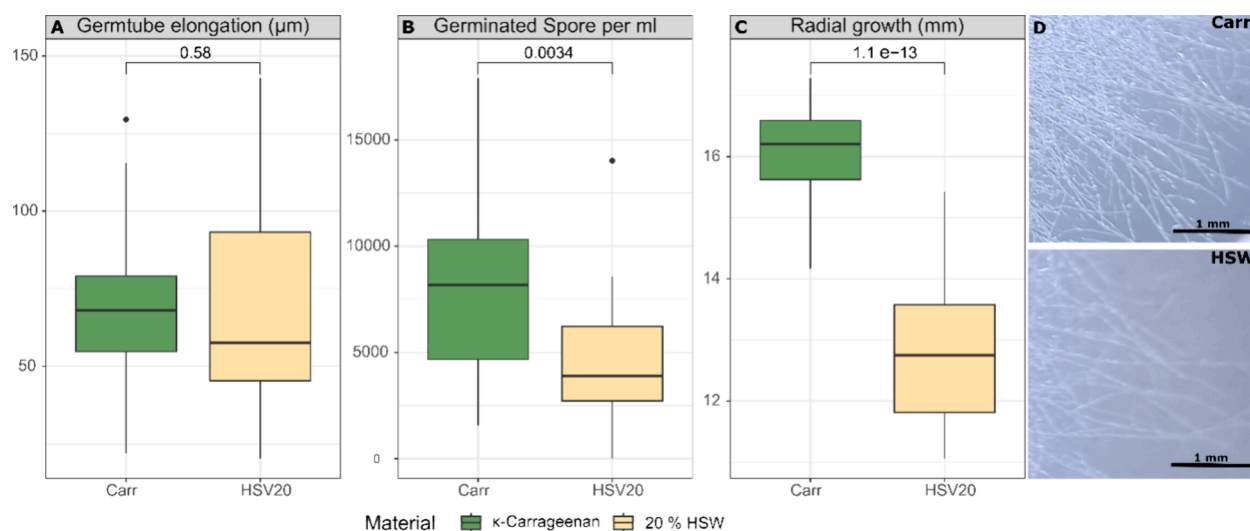


**Figure 10.** Response of *F. solani* mycelium growth, elongation, and germination rate grown on (A) carrageenan and (B) 20% CHSW and (D) microscopic observations of *F. solani* growth in Carr (upper) and 20% HSW (bottom).

structure with a noticeable swelling ability of superabsorbent hydrogels, allowing them to absorb large quantities of water when tested in three different liquid media. The hydrogels containing 20 wt % of HSW stand out because of their superior properties. They reached the greatest swelling after 24 h: 5242% in deionized H<sub>2</sub>O, 5345% in tap H<sub>2</sub>O and 5242% in fertilizer solution. Additionally, these hydrogels swelled 5000% within just 5 h when immersed in an aqueous fertilizer solution. Moreover, this type of hydrogel demonstrated good mechanical properties and potential as a complete alternative for soilless cultivation, supporting seedling growth without degrading or exhibiting toxicity, maintaining optimal hydration, and showing biostimulant properties. Plant growth experiment showed that hydrogels with HSW promoted the development of *A. thaliana* seedlings compared to the nonhydrolyzed system, producing plants with greater fresh and dry weight, a root system with more secondary roots, and an apical area free from stress signs, such as premature flowering. The results also showed a potential fungicidal impact of the hydrolyzed gel on plant root pathogens.

Overall, this proof-of-concept study may be a valuable contribution to soilless cultivation and sustainable agriculture, where biobased hydrogels serve as growth substrates without harming ecosystems while optimizing available resources. In the future, testing new types of seaweed hydrolytes and conducting trials with edible plants could further evaluate the suitability of these composites for specific crops.

## ■ ASSOCIATED CONTENT

### SI Supporting Information

The Supporting Information is available free of charge at <https://pubs.acs.org/doi/10.1021/acsagstech.4c00723>.

FTIR spectra of A: HSW, 10 HSW, 30 HSW, 50 HSW and B: 5 WSW, 10 WSW, 30 WSW, 50 WSW (Figure S1); XRD patterns of A: 5 HSW (a), 10 HSW (b), 30 HSW (c), 50 HSW (d); B: 5 WSW (a), 10 WSW (b), 30 WSW (c), 50 WSW (d) (Figure S2); SEM (Figure S3); EDS (Figure S4); images of *A. thaliana* seedlings (Figure S5) (PDF)

## ■ AUTHOR INFORMATION

### Corresponding Authors

**Camilla Febo** – Faculty of Agricultural, Environmental and Food Sciences, Free University of Bolzano, 39100 Bolzano, Italy; Faculty of Engineering, Free University of Bolzano, 39100 Bolzano, Italy; Italian Institute of Technology, 16163 Genova, Italy; [orcid.org/0000-0002-6935-5286](https://orcid.org/0000-0002-6935-5286); Email: [Camilla.Febo@student.unibz.it](mailto:Camilla.Febo@student.unibz.it)

**Athanassia Athanassiou** – Italian Institute of Technology, 16163 Genova, Italy; [orcid.org/0000-0002-6533-3231](https://orcid.org/0000-0002-6533-3231); Email: [Athanassia.athanassiou@iit.it](mailto:Athanassia.athanassiou@iit.it)

**Danila Merino** – Italian Institute of Technology, 16163 Genova, Italy; Present Address: Sustainable Biocomposite Materials, Basque Center for Macromolecular Design and Engineering (POLYMAT), University of the Basque Country (UPV-EHU), Tolosa Avenue, 72, 20018 Donostia-San Sebastián, Spain; [orcid.org/0000-0002-5098-8550](https://orcid.org/0000-0002-5098-8550); Email: [danila.merino@ehu.eus](mailto:danila.merino@ehu.eus)

### Authors

**Manuela Ciocca** – Faculty of Engineering, Free University of Bolzano, 39100 Bolzano, Italy

**Mauro Maver** – Competence Centre for Plant Health, 39100 Bolzano, Italy; [orcid.org/0000-0002-8162-3618](https://orcid.org/0000-0002-8162-3618)

**Tanja Mimmo** – Faculty of Agricultural, Environmental and Food Sciences, Free University of Bolzano, 39100 Bolzano, Italy; Competence Centre for Plant Health, 39100 Bolzano, Italy

**Oussama Bouaicha** – Faculty of Agricultural, Environmental and Food Sciences, Free University of Bolzano, 39100 Bolzano, Italy

**Luigimaria Borruso** – Faculty of Agricultural, Environmental and Food Sciences, Free University of Bolzano, 39100 Bolzano, Italy

**Paolo Lugli** – Faculty of Engineering, Free University of Bolzano, 39100 Bolzano, Italy

**Luisa Petti** – Faculty of Engineering, Free University of Bolzano, 39100 Bolzano, Italy; Competence Centre for Plant Health, 39100 Bolzano, Italy; [orcid.org/0000-0003-0264-7185](https://orcid.org/0000-0003-0264-7185)

Complete contact information is available at:

<https://pubs.acs.org/10.1021/acsagst.4c00723>

### Author Contributions

A.A., L.P., and D.M. conceptualized and designed the experiments; C.F. and O.B. performed the experiments; C.F., D.M., and A.A. analyzed the data and results, C.F. and D.M. wrote and edited the manuscript. P.L., L.P., and A.A. supervised and provided resources. All authors agreed with the final version of the manuscript. A.A. and D.M. jointly directed this study.

### Notes

The authors declare no competing financial interest.

### ACKNOWLEDGMENTS

The authors would like to thank Simone Lauciello for acquiring SEM pictures.

### REFERENCES

- (1) *Water for Prosperity and Peace Water for Prosperity and Peace The United Nations World Water Development Report 2024*; 2024.
- (2) Orsini, F.; Gasperi, D.; Marchetti, L.; Piovene, C.; Draghetti, S.; Ramazzotti, S.; Bazzocchi, G.; Gianquinto, G. Exploring the Production Capacity of Rooftop Gardens (RTGs) in Urban Agriculture: The Potential Impact on Food and Nutrition Security, Biodiversity and Other Ecosystem Services in the City of Bologna. *Food Secur* **2014**, *6* (6), 781–792.
- (3) Van Veenhuizen, R. *Urban Agriculture for Green and Productive Cities Urban Agriculture for Green and Productive Cities*; 1930.
- (4) Zhao, Z.; Xu, T.; Pan, X.; Susanti; White, J. C.; Hu, X.; Miao, Y.; Demokritou, P.; Ng, K. W. Sustainable Nutrient Substrates for Enhanced Seedling Development in Hydroponics. *ACS Sustain Chem. Eng.* **2022**, *10* (26), 8506–8516.
- (5) Madrid-Aispuro, R. E.; Prieto-Ruiz, J. Á.; Aldrete, A.; Hernández-Díaz, J. C.; Wehenkel, C.; Chávez-Simental, J. A.; Mexal, J. G. Alternative Substrates and Fertilization Doses in the Production of *Pinus Cembroides* Zucc. in Nursery. *Forests* **2020**, *11* (1), 71.
- (6) Draguhn, C.; Ciarimboli, N. *Peat: Formation, Uses and Biological Effects*; Nova Science Publishers: 2012.
- (7) Martínez, P.-F.; Roca, D. *Sustratos Para El Cultivo Sin Suelo. Materiales, Propiedades y Manejo*; Universidad Nacional de Colombia-Facultad de Agronomía: Bogotá, 2011; pp 37–78.
- (8) Guilherme, M. R.; Aouada, F. A.; Fajardo, A. R.; Martins, A. F.; Paulino, A. T.; Davi, M. F. T.; Rubira, A. F.; Muniz, E. C. Superabsorbent Hydrogels Based on Polysaccharides for Application in Agriculture as Soil Conditioner and Nutrient Carrier: A Review. *Eur. Polym. J.* **2015**, *72*, 365–385.
- (9) Rather, R. A.; Bhat, M. A.; Shalla, A. H. An Insight into Synthetic and Physiological Aspects of Superabsorbent Hydrogels Based on Carbohydrate Type Polymers for Various Applications: A Review. *Carbohydrate Polymer Technologies and Applications* **2022**, *3*, No. 100202.
- (10) Merino, D.; Mansilla, A. Y.; Salcedo, M. F.; Athanassiou, A. Upcycling Orange Peel Agricultural Waste for the Preparation of Green Hydrogels as Active Soil Conditioners. *ACS Sustain Chem. Eng.* **2023**, *11* (29), 10917–10928.
- (11) Skrzypczak, D.; Jarzembowski, Ł.; Izydorczyk, G.; Mikula, K.; Hoppe, V.; Mielko, K. A.; Pudełko-Malik, N.; Młynarz, P.; Chojnacka, K.; Witek-Krowiak, A. Hydrogel Alginate Seed Coating as an Innovative Method for Delivering Nutrients at the Early Stages of Plant Growth. *Polymers* **2021**, *13* (23), 4233.
- (12) Merino, D.; Alvarez, V. A. Green Microcomposites from Renewable Resources: Effect of Seaweed (*Undaria Pinnatifida*) as Filler on Corn Starch–Chitosan Film Properties. *J. Polym. Environ* **2020**, *28* (2), 500–516.
- (13) Merino, D.; Salcedo, M. F.; Mansilla, A. Y.; Casalongué, C. A.; Alvarez, V. A. Development of Sprayable Sodium Alginate-Seaweed Agricultural Mulches with Nutritional Benefits for Substrates and Plants. *Waste Biomass Valorization* **2021**, *12* (11), 6035–6043.
- (14) Roupheal, Y.; Colla, G. Editorial: Biostimulants in Agriculture. *Frontiers in Plant Science* **2020**.
- (15) Savci, S. Investigation of Effect of Chemical Fertilizers on Environment. *APCBEE Procedia* **2012**, *1*, 287–292.
- (16) Battacharyya, D.; Babgohari, M. Z.; Rathor, P.; Prithiviraj, B. Seaweed Extracts as Biostimulants in Horticulture. *Scientia Horticulturae* **2015**, *196*, 39–48.
- (17) Shukla, P. S.; Borza, T.; Critchley, A. T.; Prithiviraj, B. Carrageenans from Red Seaweeds as Promoters of Growth and Elicitors of Defense Response in Plants. *Frontiers in Marine Science* **2016**.
- (18) Hassan, S. M.; Ashour, M.; Sakai, N.; Zhang, L.; Hassani, H. A.; Gaber, A.; Ammar, G. Impact of Seaweed Liquid Extract Biostimulant on Growth, Yield, and Chemical Composition of Cucumber (*Cucumis Sativus*). *Agriculture* **2021**, *11* (4), 320.
- (19) Carillo, P.; Ciarmiello, L. F.; Woodrow, P.; Corrado, G.; Chiaiese, P.; Roupheal, Y. Enhancing Sustainability by Improving Plant Salt Tolerance through Macro- and Micro-Algal Biostimulants. *Biology* **2020**, *9*, 253.
- (20) Chanthini, K.; Kumar, C. S.; Kingsley, S. J. Antifungal Activity of Seaweed Extracts against Phytopathogen *Alternaria Solani*. *J. Acad. Indus. Res.* **2012**, *1* (2), 86.
- (21) Ambika, S.; Sujatha, K. Comparative Studies on Brown, Red and Green Alga Seaweed Extracts for Their Antifungal Activity against *Fusarium Oxysporum* f.sp. *Udum* in Pigeon Pea Var. CO (Rg)7 (Cajanus Cajan (L.) Mills.). *J. Biopestic.* **2014**, *7* (2), 167–176.
- (22) Viqar, S.; Syed, E.-H.; Jehan, A.; Mohammad, A. Effect of Brown Seaweeds and Pesticides on Root Rotting Fungi and Root-Knot Nematode Infecting Tomato Roots. *J. Appl. Bot. Food Qual.* **2009**, *83*, 50–53.
- (23) Ehteshamul-Haque, S.; Baloch, G. N.; Sultana, V.; Ara, J.; Tariq, R. M.; Athar, M. Impact of Seaweeds on Fluorescent Pseudomonas and Their Role in Suppressing the Root Diseases of Soybean and Pepper. *J. Appl. Bot. Food Qual.* **2013**, *86* (1), 126–132.
- (24) Domingo, G.; Marsoni, M.; Álvarez-Viñas, M.; Torres, M. D.; Domínguez, H.; Vannini, C. The Role of Protein-Rich Extracts from *Chondrus Crispus* as Biostimulant and in Enhancing Tolerance to Drought Stress in Tomato Plants. *Plants* **2023**, *12* (4), 845.
- (25) Elshalakany, W. A. Biochemical Efficiency of *Chondrus Crispus* Aqueous Extract for Alleviating Salinity Stress in Vicia Faba L. Cv. Masr-1. *Middle East J. Agric. Res.* **2020**, *9*, 1125–1134.
- (26) Mamede, M.; Cotas, J.; Pereira, L.; Baheevandziev, K. Seaweed Polysaccharides as Potential Biostimulants in Turnip Greens Production. *Horticulturae* **2024**, *10* (2), 130.
- (27) Ferreira, M.; Salgado, J. M.; Fernandes, H.; Peres, H.; Belo, I. Potential of Red, Green and Brown Seaweeds as Substrates for Solid State Fermentation to Increase Their Nutritional Value and to Produce Enzymes. *Foods* **2022**, *11* (23), 3864.
- (28) Kulshreshtha, G.; Burlot, A. S.; Marty, C.; Critchley, A.; Hafting, J.; Bedoux, G.; Bourgoignon, N.; Prithiviraj, B. Enzyme-Assisted Extraction of Bioactive Material from *Chondrus Crispus* and *Codium Fragile* and Its Effect on Herpes Simplex Virus (HSV-1). *Mar Drugs* **2015**, *13* (1), 558–580.
- (29) Rupert, R.; Rodrigues, K. F.; Thien, V. Y.; Yong, W. T. L. Carrageenan From *Kappaphycus Alvarezii* (Rhodophyta, Solieriaceae): Metabolism, Structure, Production, and Application. *Frontiers in Plant Science* **2022**.
- (30) Chauhan, P. S.; Saxena, A. Bacterial Carrageenases: An Overview of Production and Biotechnological Applications. *3 Biotech.* **2016**, *6*, 146.
- (31) Ali, O.; Ramsubhag, A.; Jayaraman, J. Biostimulant Properties of Seaweed Extracts in Plants: Implications towards Sustainable Crop Production. *Plants* **2021**, *10*, 531.

- (32) Merino, D.; Athanassiou, A. Alkaline Hydrolysis of Biomass as an Alternative Green Method for Bioplastics Preparation: In Situ Cellulose Nanofibrillation. *Chem. Eng. J.* **2023**, *454*, No. 140171.
- (33) Das, S. N.; Dutta, S.; Kondreddy, A.; Chilukoti, N.; Pullabhotla, S. V. S. R. N.; Vadlamudi, S.; Podile, A. R. Plant Growth-Promoting Chitinolytic *Paenibacillus Elgii* Responds Positively to Tobacco Root Exudates. *J. Plant Growth Regul.* **2010**, *29* (4), 409–418.
- (34) Campo, V. L.; Kawano, D. F.; da Silva, D. B.; Carvalho, I. Carrageenans: Biological Properties, Chemical Modifications and Structural Analysis - A Review. *Carbohydr. Polym.* **2009**, *77*, 167–180.
- (35) Bouaicha, O.; Maver, M.; Mimmo, T.; Cesco, S.; Borruso, L. Microplastic Influences the Ménage à Trois among the Plant, a Fungal Pathogen, and a Plant Growth-Promoting Fungal Species. *Ecotoxicol. Environ. Saf.* **2024**, *279*, No. 116518.
- (36) Gómez-Ordóñez, E.; Rupérez, P. FTIR-ATR Spectroscopy as a Tool for Polysaccharide Identification in Edible Brown and Red Seaweeds. *Food Hydrocoll.* **2011**, *25* (6), 1514–1520.
- (37) Abou Oualid, H.; Abdellaoui, Y.; Laabd, M.; El Ouardi, M.; Brahmi, Y.; Iazza, M.; Abou Oualid, J. Eco-Efficient Green Seaweed Codium Decorticatum Biosorbent for Textile Dyes: Characterization, Mechanism, Recyclability, and Rsm Optimization. *ACS Omega* **2020**, *5* (35), 22192–22207.
- (38) Chen, Y.; Mastalerz, M.; Schimmelmann, A. Characterization of Chemical Functional Groups in Macerals across Different Coal Ranks via Micro-FTIR Spectroscopy. *Int. J. Coal Geol.* **2012**, *104*, 22–33.
- (39) Kazłowska, K.; Hsu, T.; Hou, C. C.; Yang, W. C.; Tsai, G. J. Anti-Inflammatory Properties of Phenolic Compounds and Crude Extract from *Porphyra Dentata*. *J. Ethnopharmacol.* **2010**, *128* (1), 123–130.
- (40) Szymanska-Chargot, M.; Zdunek, A. Use of FT-IR Spectra and PCA to the Bulk Characterization of Cell Wall Residues of Fruits and Vegetables Along a Fraction Process. *Food Biophys.* **2013**, *8* (1), 29–42.
- (41) Pereira, L.; Amado, A. M.; Critchley, A. T.; van de Velde, F.; Ribeiro-Claro, P. J. A. Identification of Selected Seaweed Polysaccharides (Phycocolloids) by Vibrational Spectroscopy (FTIR-ATR and FT-Raman). *Food Hydrocoll.* **2009**, *23* (7), 1903–1909.
- (42) Mecozzi, M.; Pietroletti, M.; Scarpiniti, M.; Acquistucci, R.; Conti, M. E. Monitoring of Marine Mucilage Formation in Italian Seas Investigated by Infrared Spectroscopy and Independent Component Analysis. *Environ. Monit. Assess.* **2012**, *184* (10), 6025–6036.
- (43) Mallamace, F.; Corsaro, C.; Mallamace, D.; Vasi, S.; Vasi, C.; Dugo, G. The Role of Water in Protein's Behavior: The Two Dynamical Crossovers Studied by NMR and FTIR Techniques. *Comput. Struct. Biotechnol. J.* **2015**, *13*, 33–37.
- (44) Moniha, V.; Alagar, M.; Selvasekarapandian, S.; Sundaresan, B.; Boopathi, G. Conductive Bio-Polymer Electrolyte Iota-Carrageenan with Ammonium Nitrate for Application in Electrochemical Devices. *J. Non Cryst. Solids* **2018**, *481*, 424–434.
- (45) Sousa, A. M. M.; Morais, S.; Abreu, M. H.; Pereira, R.; Sousa-Pinto, I.; Cabrita, E. J.; Delerue-Matos, C.; Gonçalves, M. P. Structural, Physical, and Chemical Modifications Induced by Microwave Heating on Native Agar-like Galactans. *J. Agric. Food Chem.* **2012**, *60* (19), 4977–4985.
- (46) Arockia Mary, I.; Selvanayagam, S.; Selvasekarapandian, S.; Srikumar, S. R.; Ponraj, T.; Moniha, V. Lithium Ion Conducting Membrane Based on K-Carrageenan Complexed with Lithium Bromide and Its Electrochemical Applications. *Ionics (Kiel)* **2019**, *25* (12), 5839–5855.
- (47) Pereira, L.; Gheda, S. F.; Ribeiro-Claro, P. J. A. Analysis by Vibrational Spectroscopy of Seaweed Polysaccharides with Potential Use in Food, Pharmaceutical, and Cosmetic Industries. *International Journal of Carbohydrate Chemistry* **2013**, *2013*, 1–7.
- (48) Christopher Selvin, P.; Perumal, P.; Selvasekarapandian, S.; Monisha, S.; Boopathi, G.; Leena Chandra, M. V. Study of Proton-Conducting Polymer Electrolyte Based on K-Carrageenan and NH<sub>4</sub>SCN for Electrochemical Devices. *Ionics (Kiel)* **2018**, *24* (11), 3535–3542.
- (49) Martínez-Sanz, M.; Gómez-Mascaraque, L. G.; Ballester, A. R.; Martínez-Abad, A.; Brodkorb, A.; López-Rubio, A. Production of Unpurified Agar-Based Extracts from Red Seaweed *Gelidium Sesquipedale* by Means of Simplified Extraction Protocols. *Algal Res.* **2019**, *38*, No. 101420.
- (50) Ma, L.; Chai, C.; Wu, W.; Qi, P.; Liu, X.; Hao, J. Hydrogels as the Plant Culture Substrates: A Review. *Carbohydr. Polym.* **2023**, *305*, No. 120544.
- (51) Gürkan Polat, T.; Duman, O.; Tunç, S. Preparation and Characterization of Environmentally Friendly Agar/ $\kappa$ -Carrageenan/Montmorillonite Nanocomposite Hydrogels. *Colloids Surf., A* **2020**, *602*, No. 124987.
- (52) Nourmohammadi, J.; Roshanfar, F.; Farokhi, M.; Haghbin Nazarpak, M. Silk Fibroin/Kappa-Carrageenan Composite Scaffolds with Enhanced Biomimetic Mineralization for Bone Regeneration Applications. *Materials Science and Engineering C* **2017**, *76*, 951–958.
- (53) Meena, R.; Prasad, K.; Siddhanta, A. K. Development of a Stable Hydrogel Network Based on Agar-Kappa-Carrageenan Blend Cross-Linked with Genipin. *Food Hydrocoll.* **2009**, *23* (2), 497–509.
- (54) Muthulakshmi, L.; Pavithra, U.; Sivaranjani, V.; Balasubramanian, N.; Sakthivel, K. M.; Pruncu, C. I. A Novel Ag/Carrageenan–Gelatin Hybrid Hydrogel Nanocomposite and Its Biological Applications: Preparation and Characterization. *J. Mech. Behav. Biomed. Mater.* **2021**, *115*, No. 104257.
- (55) Mozaffari, E.; Tanhaei, B.; Khajenoori, M.; Movaghar Khoshkho, S. Unveiling the Swelling Behavior of  $\kappa$ -Carrageenan Hydrogels: Influence of Composition and Physiological Environment on Drug Delivery Potential. *Journal of Industrial and Engineering Chemistry* **2025**, *141*, 217.
- (56) Liu, S.; Li, L. Recoverable and Self-Healing Double Network Hydrogel Based on  $\kappa$ -Carrageenan. *ACS Appl. Mater. Interfaces* **2016**, *8* (43), 29749–29758.
- (57) Moustafa, M.; Abu-Saied, M. A.; Taha, T. H.; Elnouby, M.; El Desouky, E. A.; Alamri, S.; Shati, A.; Alrumman, S.; Alghamdii, H.; Al-Khatani, M.; Al-Qathanin, R.; Al-Emam, A. Preparation and Characterization of Super-Absorbing Gel Formulated from  $\kappa$ -Carrageenan–Potato Peel Starch Blended Polymers. *Polymers* **2021**, *13* (24), 4308.
- (58) Wada, K. C.; Takeno, K. Stress-Induced Flowering. *Plant Signal Behav.* **2010**, *5* (8), 944–947.
- (59) Teng, Z.; Luo, Y.; Pearlstein, D. J.; Zhou, B.; Johnson, C. M.; Wang, Q.; Fonseca, J. Agarose Hydrogel Composite Supports Microgreen Cultivation with Enhanced Porosity and Continuous Water Supply under Terrestrial and Microgravitational Conditions. *Int. J. Biol. Macromol.* **2022**, *220*, 135–146.
- (60) Tang, H.; Zhang, L.; Hu, L.; Zhang, L. Application of Chitin Hydrogels for Seed Germination, Seedling Growth of Rapeseed. *J. Plant Growth Regul.* **2014**, *33* (2), 195–201.
- (61) Zhang, H.; Yang, M.; Luan, Q.; Tang, H.; Huang, F.; Xiang, X.; Yang, C.; Bao, Y. Cellulose Anionic Hydrogels Based on Cellulose Nanofibers As Natural Stimulants for Seed Germination and Seedling Growth. *J. Agric. Food Chem.* **2017**, *65* (19), 3785–3791.
- (62) Farghl, A. A. M.; El-Sheekh, M. M.; El-Shahir, A. A. Seaweed Extracts as Biological Control of Aflatoxins Produced by *Aspergillus Parasiticus* and *Aspergillus Flavus*. *Egypt. J. Biol. Pest Control* **2023**, *33* (1), 50.
- (63) Ambika, S.; Sujatha, K. Antifungal Activity of Aqueous and Ethanol Extracts of Seaweeds against Sugarcane Red Rot Pathogen (*Colletotrichum Falcatum*). *Sci. Res. Essays* **2015**, *10* (6), 232–235.